Circulation Research
JOURNAL OF THE AMERICAN HEART ASSOCIATION

Calcium Phosphate Crystals Induce Cell Death in Human Vascular Smooth Muscle Cells: A Potential Mechanism in Atherosclerotic Plaque Destabilization

Alexandra E. Ewence, Martin Bootman, H. Llewelyn Roderick, Jeremy N. Skepper, Geraldine McCarthy, Matthias Epple, Markus Neumann, Catherine M. Shanahan and Diane Proudfoot

Circ Res. 2008;103:e28-e34; originally published online July 31, 2008;
doi: 10.1161/CIRCRESAHA.108.181305
Circulation Research is published by the American Heart Association, 7272 Greenville Avenue, Dallas, TX 75231

Print ISSN: 0009-7330. Online ISSN: 1524-4571

UltraRapid Communication

Calcium Phosphate Crystals Induce Cell Death in Human Vascular Smooth Muscle Cells

A Potential Mechanism in Atherosclerotic Plaque Destabilization

Alexandra E. Ewence, Martin Bootman, H. Llewelyn Roderick, Jeremy N. Skepper, Geraldine McCarthy, Matthias Epple, Markus Neumann, Catherine M. Shanahan, Diane Proudfoot

Abstract—Vascular calcification is associated with an increased risk of myocardial infarction; however, the mechanisms linking these 2 processes are unknown. Studies in macrophages have suggested that calcium phosphate crystals induce the release of proinflammatory cytokines; however, no studies have been performed on the effects of calcium phosphate crystals on vascular smooth muscle cell function. In the present study, we found that calcium phosphate crystals induced cell death in human aortic vascular smooth muscle cells with their potency depending on their size and composition. Calcium phosphate crystals of approximately 1 μm or less in diameter caused rapid rises in intracellular calcium concentration, an effect that was inhibited by the lysosomal proton pump inhibitor, bafilomycin A1. Bafilomycin A1 also blocked vascular smooth muscle cell death suggesting that crystal dissolution in lysosomes leads to an increase in intracellular calcium levels and subsequent cell death. These studies give novel insights into the bioactivity of calcified deposits and suggest that small calcium phosphate crystals could destabilize atherosclerotic plaques by initiating inflammation and by causing vascular smooth muscle cell death. **(*Circ Res.* 2008;103:e28-e34.)**

Key Words: apoptosis ■ atherosclerosis ■ calcification ■ vascular smooth muscle cells

Vascular calcification is a common finding in aging, diabetes, chronic renal failure, and atherosclerosis. Although calcium deposition is used as a diagnostic marker for atherosclerosis and is associated with an increased risk of myocardial infarction, its link with plaque rupture remains controversial. Although some histological studies suggest that calcification leads to plaque instability,[1] other biomechanical studies demonstrated no effect on plaque rupture.[2] Indeed, it has been suggested that a highly calcified fibrous cap may create a barrier that protects plaque from rupture.[3] Interestingly, investigations into the size and distribution of calcified deposits in atherosclerotic plaques have suggested that small, diffuse, "speckled," or "spotty" deposits cause local plaque stress and plaque instability,[4–6] whereas large plate-like areas of calcification correlate with stable plaques. Why these small calcific deposits should be preferentially associated with plaque rupture is unknown.

Some clues as to the mechanisms involved in calcium phosphate crystal-induced plaque instability come from studies in synovial tissue, in which calcium phosphate crystals are known to be damaging.[7] The crystals are engulfed by fibroblasts and a subsequent rise in intracellular calcium triggers a multitude of downstream effects, including matrix metalloprotease production. In macrophages, the crystals cause proinflammatory effects. Important studies in human monocyte/macrophages have recently demonstrated that small, phagocytosable basic calcium phosphate crystals were more potent in inducing the release of tumor necrosis factor-α compared with larger particles.[8,9] These studies suggested that microcalcific deposits in early stages of atherosclerosis pose a greater inflammatory risk to the plaque than macroscopically or radiologically visible deposits present in more advanced lesions. However, these studies did not address whether the different types of mineral present in the plaque, which include hydroxyapatite, carbonated hydroxyapatite, and amorphous calcium phosphate have differential effects on cell activation.[10–12] Due to the protective role of VSMCs in plaque rupture[13] and the association of small crystals with destabilized plaques, we aimed to determine whether different types and sizes of calcium phosphate crystals, including atherosclerotic vessel-derived crystals, could affect VSMC function.

Original received June 13, 2008; revision received July 21, 2008; accepted July 22, 2008.

From the Division of Cardiovascular Medicine (A.E.E., D.P.), University of Cambridge, Addenbrooke's Hospital, Cambridge, UK; the Laboratory of Molecular Signalling (M.B., H.L.R.), The Babraham Institute, Babraham, Cambridge, UK; the Department of Anatomy (J.N.S.), Multi-Imaging Centre, University of Cambridge, Cambridge, UK; the Department of Clinical Pharmacology (G.M.), Royal College of Surgeons in Ireland, Dublin, UK; Inorganic Chemistry (M.E., M.N.), University of Duisburg-Essen, Essen, Germany; and Kings College London (C.M.S.), Cardiovascular Division, James Black Centre, London, UK; and the Department of Pharmacology (H.L.R.), University of Cambridge, UK.

Correspondence to Diane Proudfoot, Department of Medicine, University of Cambridge, ACCI Building, Level 6, Box 110, Addenbrooke's Hospital, Hills Road, Cambridge CB2 2QQ, UK. E-mail dianeproudfoot@gmail.com

Circulation Research **is available at http://circres.ahajournals.org** **DOI: 10.1161/CIRCRESAHA.108.181305**

Materials and Methods

Crystals and Particles

Crystals Extracted From Atherosclerotic Tissue

Crystals were prepared from samples of human carotid arteries removed by endarterectomy from 3 different donors: a 61-year-old man, a 64-year-old woman, and a 55-year-old man. The hardened, obviously calcified regions were dissected from other areas of the atherosclerotic vessels and digested with collagenase (3 mg/mL) and elastase (1 mg/mL) overnight at 37°C. After digestion, the crystals were washed 3 times in Hanks' Balanced Salt Solution. Samples were then placed on a 70-μm sieve (Gibco) and washed further. The remaining crystals (>70 μm) were crushed using a pestle and mortar into Hanks' Balanced Salt Solution, water, or serum-free M199. Washing of the crystals at this stage was achieved using ultracentrifugation at 100 000 g to capture very small particles. For scanning electron microscopy, samples were dusted onto spectroscopically pure carbon disks attached to 13-mm Cambridge scanning electron microscopy stubs and viewed uncoated in a FEI-Philips FEGSEM operated at 5 kV. The transmission electron microscopy samples were dusted onto holey carbon film grids (Agar Scientific) and viewed in a FEI Philips CM100 transmission electron microscopy operated at 100 kV. Images were recorded on Kodak 4489 cut film and scanned as .tiff files using an AGFA Duoscan. Energy dispersive x-ray microanalysis was performed as described previously.[14]

Basic Calcium Phosphate

Basic calcium phosphate (BCP) crystals were synthesized by alkaline hydrolysis of brushite using previously described methods.[15] Mineral prepared by this method has previously been shown to have a calcium/phosphate molar ratio of 1.59 and contains partially carbonate-substituted hydroxyapatite mixed with octacalcium phosphate as determined by Fourier transform infrared spectroscopy. The crystals were weighed into vials and rendered pyrogen-free by heating at 200°C for 90 minutes. Heating has previously been shown not to alter the crystal character or the relationship of hydroxyapatite or octacalcium phosphate as confirmed by x-ray diffraction and Fourier transform infrared spectroscopy. Sonication gave crystal sizes of approximately 1 μm in diameter.

Nanoparticulate Apatite

Synthetic nanoparticulate particles were prepared as described previously.[16] These samples consisted of nanocrystalline-carbonated apatite ($Ca:PO_4^{3-}$ molar ratio 1.57:1), nanocrystalline carbonated apatite ($Ca:PO_4^{3-}$ molar ratio 1.39:1), nanocrystalline carbonate-free apatite ($Ca:PO_4^{3-}$ molar ratio 1.34:1), and amorphous carbonate-free apatite ($Ca:PO_4^{3-}$ molar ratio 1.23:1). These particles ranged from 100 to 300 nm in diameter.

Polystyrene latex beads (1 μm diameter; Fluka 89904) were used as a control particle.

All crystal preparations and beads were maintained under sterile conditions and sonicated in serum-free medium199 before use.

Cell Culture

The culture medium used was M199 (Gibco) buffered with 3.7 mg/mL $NaHCO_3$ and 5% CO_2 and supplemented with 100 IU/mL penicillin (Sigma), 100 mg/mL streptomycin, 250 ng/mL amphotericin, and 4 mmol/L of L-glutamine (Sigma). Heat-inactivated fetal calf serum (FCS) was purchased from Gibco. Human VSMCs were obtained from nonatherosclerotic areas of aortas from organ donors of various ages (both males and females, age ranged from 15 to 65 years). The cells were prepared from explants of the medial layer of aortic tissue and were confirmed as smooth muscle cells by positive staining with monoclonal antibodies against α-smooth muscle actin (A2547; Sigma). Cells were maintained in M199 medium containing 20% FCS and were used between passage 3 and 15.

Cell Viability Assay

Cell viability was measured by assessing mitochondrial activity of VSMCs using an MTT kit (Sigma). VSMCs were plated in 96-well plates at a density of 5000 cells/well in growth medium. After 16 hours, the medium was changed to 5% FCS/M199 with or without crystals and the incubation continued for 72 hours. The MTT solution (5 mg/mL MTT in RPMI-1640 without phenol red) was added to the culture solution to a volume equal to 10%. Further incubation at 37°C for 3 hours yielded purple MTT formazan crystals. Once solubilized with MTT solvent (0.1 N HCl in anhydrous isopropanol; Sigma), the absorbance in each well was measured at 570 nm with the background (650 nm) subtracted.

Detection of Apoptosis

Time-lapse videomicroscopy was used to determine whether cells exposed to crystals underwent apoptosis through the classical cell membrane "blebbing" and subsequent cell fragmentation. VSMCs were plated in 12-well dishes at 40 000 cells per well in growth medium. After an overnight incubation at 37°C, the medium was changed to 0.5% FCS/M199 with or without crystals gassed in 5% CO_2 for 30 minutes before being sealed. Images were captured digitally every 10 minutes for 24 hours.

Additionally, VSMCs were plated in 4-well chamber slides, 10 000 cells per well in growth medium. After an overnight incubation, the medium was changed to 0.5% FCS/M199 with or without crystals. Crystals were incubated with VSMCs for up to 24 hours, washed in phosphate-buffered saline, fixed in 4% formaldehyde/phosphate-buffered saline, and mounted in Mowiol (containing DAPI). Apoptotic cells were identified by their bright, condensed, punctuate, or fragmented nuclear morphology.

Proliferation Assay

VSMCs were plated in 24-well plates at a density of 10 000 cells/well in growth medium and allowed to attach overnight for 16 hours. The medium was then changed to 0.5% FCS/M199 to induce quiescence. After 72 hours in 0.5% FCS, the medium was replaced by 5% FCS/M199 with or without addition of crystals. Cells were counted after trypsinization using a hemocytometer.

Measurement of Intracellular Calcium ($[Ca^{2+}]_i$)

Measurement of cytosolic calcium was performed by monitoring Fura-2 fluorescence of VSMCs adhered to glass coverslips using a Perkin Elmer imaging system. Fura-2 was loaded into the cells by incubation with 2 μmol/L Fura-2 acetoxymethyl ester (30 minutes incubation followed by a 30-minute period for de-esterification) in physiological buffer (NaCl, 121 mmol/L; KCl, 5.4 mmol/L; $MgCl_2$, 0.8 mmol/L; $CaCl_2$, 1.8 mmol/L; $NaHCO_3$, 6 mmol/L; D-glucose, 5.5 mmol/L; Hepes, 25 mmol/L; pH 7.3). A single glass coverslip with adherent cells was mounted on the stage of a Nikon TE200 inverted epifluorescence microscope coupled to a xenon arc lamp (Nikon) light source in a temperature-controlled chamber (37°C) and sealed to eliminate evaporation after addition of agonists/crystals. Fluorescence images were obtained with alternate excitation at 340 and 380 nm, which were selected using a Sutter filter wheel (Sutter Industries). Emitted light was filtered at wavelengths >510 nm and collected by a Hammamatsu Orca ER camera. The acquired images were stored and subsequently processed offline with Ultraview software (Perkin Elmer Life Sciences Ltd, Cambridge, UK).

The Fura-2/propidium iodide measurements were obtained using an Olympus CellR imaging system configured around an Olympus IX81 microscope. Cells were loaded with Fura-2 as described previously and placed on the stage of the microscope. Propidium iodide (0.5 μg/mL) was added to the extracellular solution at the start of the experiment. The cells were alternately excited at 340 nm (to monitor calcium) and 490 nm (to monitor propidium iodide) with emitted light being collected at >500 nm and >515 nm, respectively. The fluorescence images were captured using a Hammamatsu Orca ER camera. Analysis of changes in Fura-2 or propidium iodide fluorescence was examined offline using ImageJ software.

In some experiments, bafilomycin A1 (10 nmol/L final concentration; Sigma) was added to VSMCs 30 minutes before addition of crystals. Bafilomycin A1 (10 nmol/L) was also present during analysis.

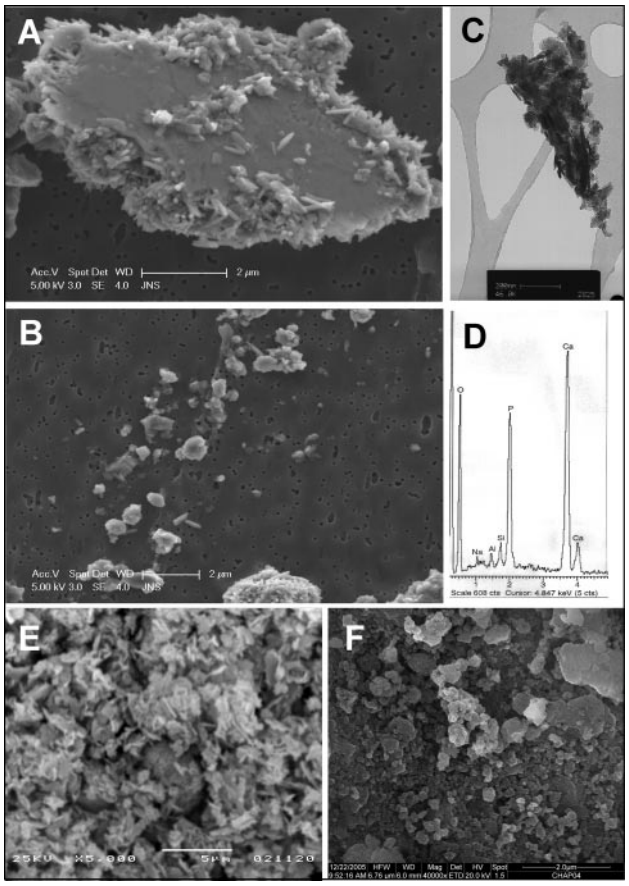

Figure 1. Crystal characteristics. A–B, Scanning electron microscopy (SEM) images of crystals isolated from human carotid atherosclerotic plaques. Crystal size ranged from approximately 50 nm to 8 μm (bar=2 μm for each image). C, Transmission electron microscopy showing a cross-section of atherosclerotic crystals (transmission electron microscopy, bar=200 nm). D, Electron dispersive x-ray spectroscopy (EDX) of atherosclerotic crystals showing that they consist of mostly calcium, phosphorous, and oxygen, consistent with an apatite-like material. E, SEM image of BCP crystals with an average particle size of 1 μm (bar=5 μm). F, SEM image of nanocrystalline carbonated apatite ($Ca:PO_4^{3-}$ molar ratio 1.57:1) that ranged in diameter from 100 to 300 nm (bar=2 μm).

Statistics

Data shown are means±SD. Comparisons between 2 means were performed using the Student *t* test.

Results

Analysis of Atherosclerotic Vessel-Derived Crystals

Electron microscopic and elemental analysis of human atherosclerotic crystals showed that they consisted of calcium phosphate and varied widely in size and morphology consistent with other studies (Figure 1).[10] The crystals ranged from approximately 50 nm to 8 μm. Although there was variation in size, these crystals fall within the same size range as the synthetic BCP (approximately 1 μm diameter) and calcium phosphate nanocrystals (ranging from 100 to 300 nm) prepared for comparative studies (Figure 1).

Effects of Calcium Phosphate Crystals on Vascular Smooth Muscle Cell Viability, Number, and Apoptosis

VSMCs were treated with synthetic calcium phosphate crystals and human atherosclerosis-derived crystals first to determine their effects on VSMC viability using an MTT assay. BCP, human crystals, and each of the nanocrystalline particles (carbonated and noncarbonated apatite) significantly reduced cell viability with amorphous carbonate-free apatite having the greatest effect (Figure 2A). To confirm that the effects seen were due to intact crystals, the crystals were incubated in culture medium at 37°C for 24 hours, subjected to ultracentrifugation, and the supernatant was added to VSMCs. This crystal-conditioned medium (carbonate-free apatite CM) did not reduce cell viability but caused a modest significant increase in VSMC viability (Figure 2A). To further confirm that cell death was not associated with crystal dissolution in the culture medium, VSMCs were cultured in media containing 3 times physiological calcium or up to 5 times the physiological level of phosphate in the presence of serum and this had no effect on VSMC cell death as previously described[17] (data not shown).

Latex beads with 1 μm diameter were used as a control particle and had no effect on VSMC viability (Figure 2A). Larger pieces of crystal (nonsonicated aggregates of >40 μm diameter) had no effect on VSMC viability (Figure 2A), suggesting that crystal size is important.

To determine if the reduction in cell viability was due to a reduction in cell number, the effects on cell growth were investigated by exposing synchronized VSMCs to BCP or human crystals in the presence of 5% FCS over a 5-day period and counting the number of VSMCs. In these experiments, cell numbers were reduced in the presence of BCP after 3 days of treatment (Figure 2B). However, the human crystals had no effect at day 3 but significantly reduced VSMC numbers after 5 days of treatment (Figure 2B). The lack of effect of human crystals at day 3 was not due to effects on proliferation of VSMCs because both BCP and human crystals had minimal effects on proliferation as measured by time-lapse videomicroscopy (data not shown). Therefore, compared with BCP, human crystals were slower in causing a reduction in cell numbers.

Using time-lapse videomicroscopy, apoptosis was significantly increased in the presence of BCP (Figure 2C). BCP and human crystals also significantly increased the numbers of condensed or fragmented nuclei seen with DAPI staining, indicative of increased VSMC apoptosis, with the human crystals again being less potent than BCP (Figure 2D).

Effects of Crystals on Intracellular Calcium ($[Ca^{2+}]_i$) Changes

Studies in synovial fibroblasts have suggested that the effects of crystals on their proliferation are due to phagocytosis of crystals, dissolution in lysosomes, and subsequent rises in intracellular calcium $[Ca^{2+}]_i$ levels.[18] Because changes in $[Ca^{2+}]_i$ levels are also associated with induction of apoptosis, we investigated whether the calcium phosphate crystals alter VSMC $[Ca^{2+}]_i$ levels. We found that the addition of BCP crystals to VSMCs caused a rapid rise in $[Ca^{2+}]_i$ (Figure 3A).

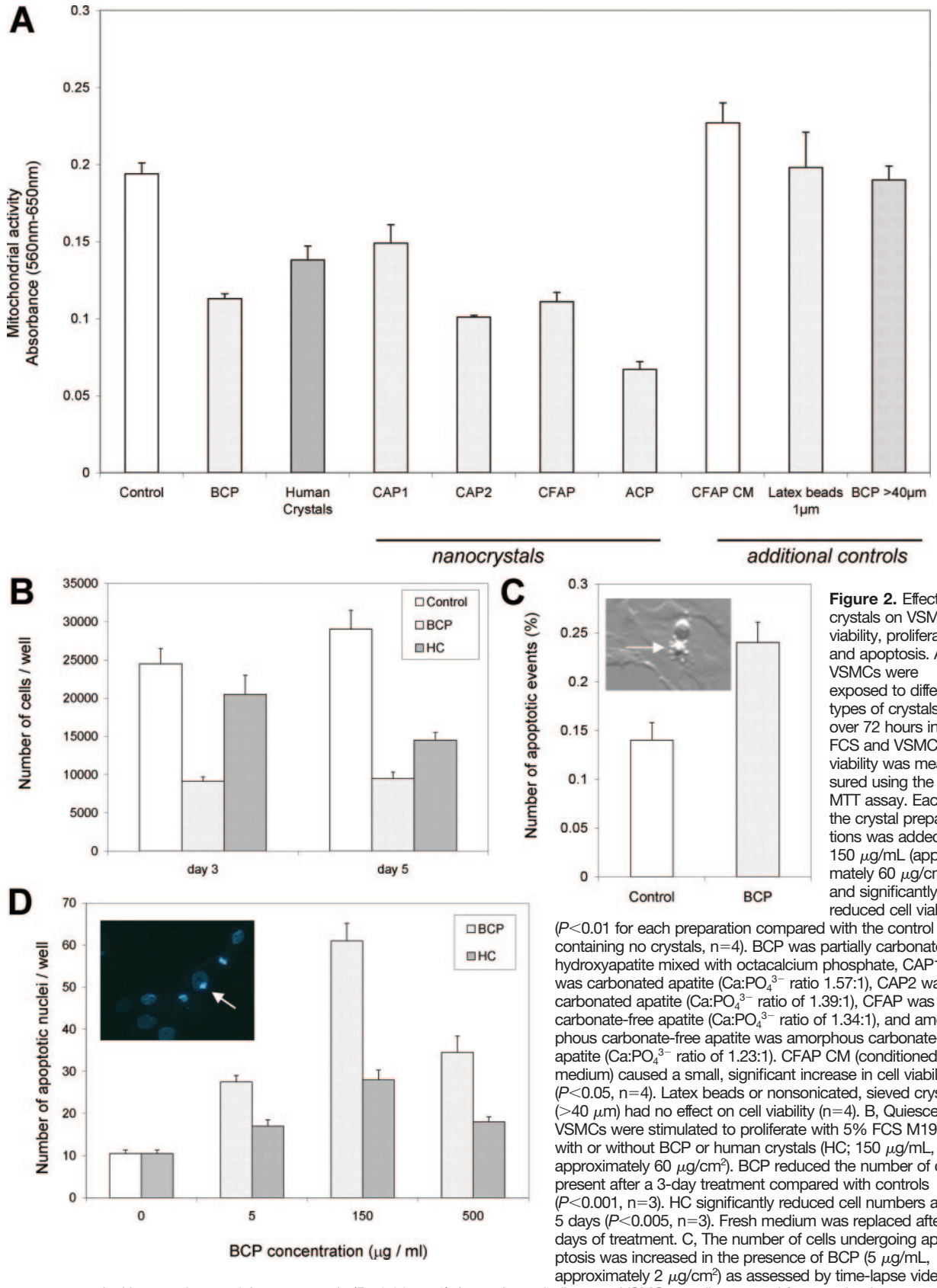

Figure 2. Effect of crystals on VSMC viability, proliferation, and apoptosis. A, VSMCs were exposed to different types of crystals over 72 hours in 5% FCS and VSMC viability was measured using the MTT assay. Each of the crystal preparations was added at 150 μg/mL (approximately 60 μg/cm^2) and significantly reduced cell viability ($P<0.01$ for each preparation compared with the control containing no crystals, n=4). BCP was partially carbonated hydroxyapatite mixed with octacalcium phosphate, CAP1 was carbonated apatite (Ca:PO_4^{3-} ratio 1.57:1), CAP2 was carbonated apatite (Ca:PO_4^{3-} ratio of 1.39:1), CFAP was carbonate-free apatite (Ca:PO_4^{3-} ratio of 1.34:1), and amorphous carbonate-free apatite was amorphous carbonate-free apatite (Ca:PO_4^{3-} ratio of 1.23:1). CFAP CM (conditioned medium) caused a small, significant increase in cell viability ($P<0.05$, n=4). Latex beads or nonsonicated, sieved crystals (>40 μm) had no effect on cell viability (n=4). B, Quiescent VSMCs were stimulated to proliferate with 5% FCS M199 with or without BCP or human crystals (HC; 150 μg/mL, approximately 60 μg/cm^2). BCP reduced the number of cells present after a 3-day treatment compared with controls ($P<0.001$, n=3). HC significantly reduced cell numbers after 5 days ($P<0.005$, n=3). Fresh medium was replaced after 3 days of treatment. C, The number of cells undergoing apoptosis was increased in the presence of BCP (5 μg/mL, approximately 2 μg/cm^2) as assessed by time-lapse videomicroscopy compared with controls containing no crystals ($P<0.01$, n=3). Inset, Arrow indicates a VSMC rounding up and fragmenting into apoptotic bodies. D, BCP and human crystals increased numbers of VSMC condensed or fragmented nuclei using DAPI (inset image) with maximal effects seen with the 150-μg/mL dose (approximately 60 μg/cm^2; $P<0.01$ for each concentration tested compared with controls, n=4). Inset, Arrow indicates a VSMC nucleus with a bright, condensed area suggesting this is an apoptotic cell.

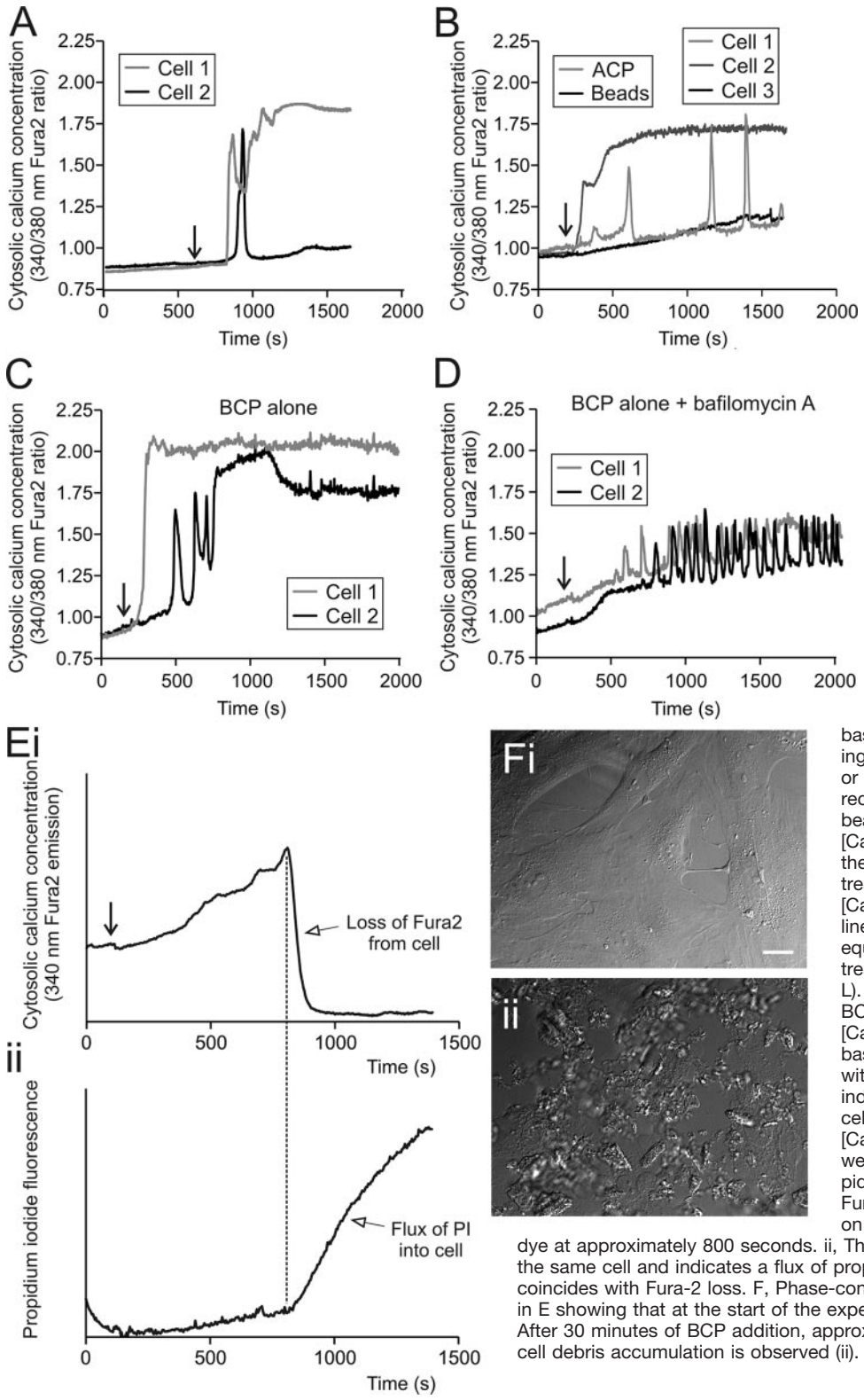

Figure 3. VSMC calcium response to calcium phosphate crystals. A, Representative traces of $[Ca^{2+}]_i$ changes in VSMCs stimulated with BCP (150 μg/mL, approximately 60 μg/mL). Addition of BCP is indicated by the arrow (at 600 seconds). Two distinct types of responses to BCP were observed, a sharp rise in $[Ca^{2+}]_i$ that showed no recovery (as for cell 1) or a sharp rise in $[Ca^{2+}]_i$ followed by recovery to baseline (cell 2). Cells that showed no recovery to baseline died (cell 1) as monitored by loss of Fura-2 dye from the cells. This image represents data from an experiment in which 21 cells were monitored, 11 of which went on to die. A total of 91 cells in 8 separate experiments displayed these $[Ca^{2+}]_i$ patterns, 44 of which died. B, Representative traces of $[Ca^{2+}]_i$ changes in VSMCs stimulated with amorphous calcium phosphate (ACP) and latex beads, both at a final concentration of 150 μg/mL, approximately 60 μg/cm^2. ACP induced either a sharp rise in $[Ca^{2+}]_i$ followed by recovery to baseline (cell 1, light gray line displaying cyclic transient changes in $[Ca^{2+}]_i$) or a sharp rise in $[Ca^{2+}]_i$ with no recovery (cell 2, dark gray line). Latex beads (black line) had no effects on $[Ca^{2+}]_i$. C, Representative traces of the calcium response of 2 VSMCs treated with BCP showing rises in $[Ca^{2+}]_i$ that did not recover to baseline. D, Representative traces of 2 equivalent VSMCs to those in C, pretreated with bafilomycin A1 (10 nmol/L). In the presence of bafilomycin A1, BCP caused small, oscillatory rises in $[Ca^{2+}]_i$. and all cells recovered to baseline with no cell death compared with approximately 50% cell death induced with BCP alone in equivalent cells. Bafilomycin A1 had no effect on $[Ca^{2+}]_i$ when added alone. E, VSMCs were loaded with Fura-2 and propidium iodide. i, The emission of Fura-2 in one of the VSMCs that went on to die, indicating a sudden loss of dye at approximately 800 seconds. ii, The propidium iodide fluorescence in the same cell and indicates a flux of propidium iodide into the cell that coincides with Fura-2 loss. F, Phase-contrast images of the cells monitored in E showing that at the start of the experiment, cells are clearly seen (i). After 30 minutes of BCP addition, approximately half of these cells died and cell debris accumulation is observed (ii). Bar=10 μm.

These responses occurred between 20 and 600 seconds after addition of the crystals with each individual cell having its own pattern of calcium signals. However, all cells displayed one of 2 distinct responses to the crystals: (1) a sharp, sustained rise (Figure 3A, cell 1); or (2) a sharp rise followed by recovery to near baseline levels of calcium (Figure 3A, cell 2). The cells that displayed sustained rises in calcium in response to crystals rapidly lost Fura-2 dye, which was accompanied by the simultaneous accumulation of propidium iodide, indicating loss of membrane integrity (Figure 3E–F). Importantly, latex beads did not alter $[Ca^{2+}]_i$ levels (Figure 3B) and the addition of extra calcium (3 times the physiological level of calcium ions) did not affect $[Ca^{2+}]_i$ levels (data not shown).

Each of the different nanocrystalline preparations had similar effects to BCP, ie, inducing $[Ca^{2+}]_i$ rises and cell death accompanied by a loss of calcium homeostasis in approximately 50% of VSMCs and inducing transient cyclic increases in $[Ca^{2+}]_i$ levels in the remaining 50% (Figure 3B). In contrast, the human atherosclerotic crystals had little effect on $[Ca^{2+}]_i$ levels over 1 hour of analysis (data not shown). We hypothesized that like bone hydroxyapatite,[19] human atherosclerotic-derived crystals are associated with proteins, including serum proteins, that may have the capacity to alter crystal-induced calcium responses. To investigate this possibility, we incubated BCP crystals in 1% FCS before addition to VSMCs and found that they had no effect on $[Ca^{2+}]_i$ in VSMCs (data not shown), suggesting that association of calcium phosphate crystals with serum proteins can dampen their activity.

The differential effects of calcium and crystals shown previously suggested that the changes in $[Ca^{2+}]_i$ could be due to crystal uptake and subsequent release of calcium ions after acidification/dissolution of crystals in lysosomes. To test this, we used bafilomycin A1, a specific inhibitor of lysosome acidification. Bafilomycin A1 abolished the sharp rises in $[Ca^{2+}]_i$ seen with BCP treatment of VSMCs (Figure 3C–D). In the presence of bafilomycin A1, BCP failed to induce cell death over 1 hour of analysis. These results suggested that lysosomal degradation of calcium phosphate crystals was necessary in causing increased $[Ca^{2+}]_i$ and mediating cell death induced by the crystals.

Discussion

Apoptosis of plaque VSMCs has been linked with plaque rupture and instability for some time.[20] In the present study, we have identified a novel mechanism for the induction of VSMC death by calcium phosphate micro- and nanoparticles. These observations may help to explain why microcalcifications have recently been found to cause local stress in atherosclerotic fibrous caps[6] and why speckled calcified deposits are commonly found in ruptured coronary plaques.[4] In addition to weakening of the fibrous cap, VSMC death may have other downstream consequences within atherosclerotic plaques, including potentiating further calcification by providing a nidus for nucleation[21] or potentially activating various inflammatory pathways such as the release of cytokines or other novel pathways such as release of HMGB1[22–24] with further studies now required to further explore these downstream effects.

Calcium phosphate crystals have been shown to have activity in cell types other than VSMCs. For example, hydroxyapatite-containing "atherosclerotic gruel"-induced apoptosis in macrophages,[25] and calcium phosphate nanocrystals have been reported to induce apoptosis in cancer cells.[26] In synovial fibroblasts, proliferation is enhanced in the presence of calcium phosphate crystals,[7] which implies that there is some cell specificity in the response of a cell to calcium phosphate crystals. Experiments investigating the $[Ca^{2+}]_i$ response in VSMCs revealed that calcium phosphate crystals caused rapid rises in $[Ca^{2+}]_i$ in all of the cells analyzed. In approximately 50% of the cells, the $[Ca^{2+}]_i$ rises did not recover back to baseline and these cells died. Why only 50% of the cells responded in this way is intriguing. Because of the heterogeneous nature of VSMCs, it is possible that one population of VSMCs within each isolate has different calcium handling mechanisms, phagocytosis kinetics, or susceptibility to cell death. Experiments using bafilomycin A1 showed that inhibition of lysosomal proton pump activity reduced the magnitude of $[Ca^{2+}]_i$ rises and inhibited cell death induced by BCP. This suggests that calcium phosphate crystals are rapidly degraded in lysosomes and subsequent acidification leads to the release of calcium into the cell. We expect that the released calcium is initially sequestered by calcium stores or pumped out of the cell until the sustained calcium rise leads to loss of function of membrane pumps leading to cell death. The mechanism of intracellular mobilization of calcium from the lysosomes is currently unknown and could involve a number of pathways, including nicotinic acid adenine dinucleotide phosphate.[27] Further studies are required to elucidate the exact mechanisms involved in the crystal-induced $[Ca^{2+}]_i$ rise and subsequent cell death.

Scanning electron microscopy demonstrated that calcified extracts from atherosclerotic tissue contained calcium phosphate crystals of different shapes and sizes, which is in agreement with other studies.[10] We did not detect carbonated forms of crystals in our samples as seen in other studies and in our own previous in vitro studies of calcified VSMC apoptotic bodies.[21] However, synthetic carbonated or noncarbonated forms of hydroxyapatite had similar effects in reducing VSMC viability. The nanocrystals (<300 nm) and BCP (approximately 1 μm) had similar effects in reducing cell viability; however, aggregates of greater than 40 μm did not reduce cell viability. This is likely to be due to a lack of phagocytosis of larger particles and implies that small nonaggregated particles in atherosclerotic plaques may be more cytotoxic to VSMCs compared with larger deposits. These observations complement studies in macrophages in which crystals of 1 to 2 μm diameter were more potent than larger crystals (approximately 15 μm) in causing the release of proinflammatory cytokines.[9]

The crystal preparation with the greatest effect in reducing cell viability was amorphous calcium phosphate, which raises the possibility that the active regulation of calcification is designed to produce crystals similar to hydroxyapatite found in blood vessels and bone, because these are less damaging than more soluble forms of calcium phosphate. In support of this, crystals isolated from atherosclerotic tissue were less potent than synthetic crystal preparations at reducing cell viability, they were slower in reducing cell numbers, and they had little effect on calcium levels in VSMCs. The reduced potency of the human crystals may be due to having different surface properties and containing factors such as antiapoptotic and calcification-regulatory proteins (including fetuin) that may offset their detrimental effects. In support of this, in contrast to untreated BCP crystals, serum-treated BCP crystals had no effect on calcium levels in VSMCs. Indeed, VSMCs in vivo will not be exposed to pure, uncoated crystals but will meet them in the context of their associated factors and microenvironment within the plaque that may alter the kinetics of crystal phagocytosis and toxicity.

If as our study suggests, the degree of potency of crystals in inducing VSMC death is dependent on their size, composition, and associated factors, this will have important implications for how we design treatments to ameliorate plaque calcification.

Source of Funding

The research in this study was funded by the British Heart Foundation.

Disclosures

None.

References

1. Farb A, Burke AP, Tang AL, Liang TY, Mannan P, Smialek J, Virmani R. Coronary plaque erosion without rupture into a lipid core. A frequent cause of coronary thrombosis in sudden coronary death. *Circulation*. 1996; 93:1354–1363.
2. Huang H, Virmani R, Younis H, Burke AP, Kamm RD, Lee RT. The impact of calcification on the biomechanical stability of atherosclerotic plaques. *Circulation*. 2001;103:1051–1056.
3. Doherty TM, Detrano RC. Coronary arterial calcification as an active process: a new perspective on an old problem. *Calcif Tissue Int*. 1994; 54:224–230.
4. Virmani R, Burke AP, Kolodgie FD, Farb A. Pathology of the thin-cap fibroatheroma: a type of vulnerable plaque. *J Interv Cardiol*. 2003;16: 267–272.
5. Ehara S, Kobayashi Y, Yoshiyama M, Shimada K, Shimada Y, Fukuda D, Nakamura Y, Yamashita H, Yamagishi H, Takeuchi K, Naruko T, Haze K, Becker AE, Yoshikawa J, Ueda M. Spotty calcification typifies the culprit plaque in patients with acute myocardial infarction: an intravascular ultrasound study. *Circulation*. 2004;110:3424–3429.
6. Vengrenyuk Y, Carlier S, Xanthos S, Cardoso L, Ganatos P, Virmani R, Einav S, Gilchrist L, Weinbaum S. A hypothesis for vulnerable plaque rupture due to stress-induced debonding around cellular microcalcifications in thin fibrous caps. *Proc Natl Acad Sci U S A*. 2006;103: 14678–14683.
7. Morgan MP, McCarthy GM. Signaling mechanisms involved in crystal-induced tissue damage. *Curr Opin Rheumatol*. 2002;14:292–297.
8. Nadra I, Mason JC, Philippidis P, Florey O, Smythe CD, McCarthy GM, Landis RC, Haskard DO. Proinflammatory activation of macrophages by basic calcium phosphate crystals via protein kinase C and MAP kinase pathways: a vicious cycle of inflammation and arterial calcification? *Circ Res*. 2005;96:1248–1256.
9. Nadra I, Boccaccini AR, Philippidis P, Whelan LC, McCarthy GM, Haskard DO, Landis RC. Effect of particle size on hydroxyapatite crystal-induced tumor necrosis factor alpha secretion by macrophages. *Atherosclerosis*. 2008;196:98–105.
10. Schmid K, McSharry WO, Pameijer CH, Binette JP. Chemical and physicochemical studies on the mineral deposits of the human atherosclerotic aorta. *Atherosclerosis*. 1980;37:199–210.
11. Kim KM. Calcification of matrix vesicles in human aortic valve and aortic media. *Fed Proc*. 1976;35:156–162.
12. Becker A, Epple M, Muller KM, Schmitz I. A comparative study of clinically well-characterized human atherosclerotic plaques with histological, chemical, and ultrastructural methods. *J Inorg Biochem*. 2004; 98:2032–2038.
13. Iyemere VP, Proudfoot D, Weissberg PL, Shanahan CM. Vascular smooth muscle cell phenotypic plasticity and the regulation of vascular calcification. *J Intern Med*. 2006;260:192–210.
14. Proudfoot D, Skepper JN, Shanahan CM, Weissberg PL. Calcification of human vascular cells in vitro is correlated with high levels of matrix Gla protein and low levels of osteopontin expression. *Arterioscler Thromb Vasc Biol*. 1998;18:379–388.
15. Evans RW, Cheung HS, McCarty DJ. Cultured human monocytes and fibroblasts solubilize calcium phosphate crystals. *Calcif Tissue Int*. 1984; 36:645–650.
16. Welzel T, Meyer-Zaika W, Epple M. Continuous preparation of functionalised calcium phosphate nanoparticles with adjustable crystallinity. *Chem Commun (Camb)*. 2004;1204–1205.
17. Schurgers LJ, Spronk HM, Skepper JN, Hackeng TM, Shanahan CM, Vermeer C, Weissberg PL, Proudfoot D. Post-translational modifications regulate matrix Gla protein function: importance for inhibition of vascular smooth muscle cell calcification. *J Thromb Haemost*. 2007;5:2503–2511.
18. Halverson PB, Greene A, Cheung HS. Intracellular calcium responses to basic calcium phosphate crystals in fibroblasts. *Osteoarthritis Cartilage*. 1998;6:324–329.
19. Triffitt JT, Gebauer U, Ashton BA, Owen ME, Reynolds JJ. Origin of plasma alpha2HS-glycoprotein and its accumulation in bone. *Nature*. 1976;262:226–227.
20. Clarke M, Bennett M. The emerging role of vascular smooth muscle cell apoptosis in atherosclerosis and plaque stability. *Am J Nephrol*. 2006;26: 531–535.
21. Proudfoot D, Skepper JN, Hegyi L, Bennett MR, Shanahan CM, Weissberg PL. Apoptosis regulates human vascular calcification in vitro: evidence for initiation of vascular calcification by apoptotic bodies. *Circ Res*. 2000;87:1055–1062.
22. Park JS, Gamboni-Robertson F, He Q, Svetkauskaite D, Kim JY, Strassheim D, Sohn JW, Yamada S, Maruyama I, Banerjee A, Ishizaka A, Abraham E. High mobility group box 1 protein interacts with multiple Toll-like receptors. *Am J Physiol Cell Physiol*. 2006;290:C917–924.
23. Zhou Z, Han JY, Xi CX, Xie JX, Feng X, Wang CY, Mei L, Xiong WC. HMGB1 regulates RANKL-induced osteoclastogenesis in a manner dependent on RAGE. *J Bone Miner Res*. 2008;23:1084–1096.
24. Porto A, Palumbo R, Pieroni M, Aprigliano G, Chiesa R, Sanvito F, Maseri A, Bianchi ME. Smooth muscle cells in human atherosclerotic plaques secrete and proliferate in response to high mobility group box 1 protein. *Faseb J*. 2006;20:2565–2566.
25. Li W, Ostblom M, Xu LH, Hellsten A, Leanderson P, Liedberg B, Brunk UT, Eaton JW, Yuan XM. Cytocidal effects of atheromatous plaque components: the death zone revisited. *Faseb J*. 2006;20:2281–2290.
26. Chen X, Deng C, Tang S, Zhang M. Mitochondria-dependent apoptosis induced by nanoscale hydroxyapatite in human gastric cancer SGC-7901 cells. *Biol Pharm Bull*. 2007;30:128–132.
27. Zhang F, Zhang G, Zhang AY, Koeberl MJ, Wallander E, Li PL. Production of nicotinic acid adenine dinucleotide phosphate and its role in Ca2+ mobilization associated with lysosomes in coronary arterial myocytes. *Am J Physiol Heart Circ Physiol*. 2006;291:H274–282.